Current Biology, Vol. 14, 1801–1811, October 26, 2004, ©2004 Elsevier Ltd. All rights reserved. DOI 10.1016/j.cub.2004.10.002

XRHAMM Functions in Ran-Dependent Microtubule Nucleation and Pole Formation during Anastral Spindle Assembly

Aaron C. Groen,[1,2,*] Lisa A. Cameron,[2,3] Margaret Coughlin,[1] David T. Miyamoto,[1] Timothy J. Mitchison,[1,2] and Ryoma Ohi[1]
[1]Department of Systems Biology
Harvard Medical School
Boston, Massachusetts 02115
[2]Cell Division Group
Marine Biological Laboratory
Woods Hole, Massachusetts 02543
[3]Department of Biology
University of North Carolina, Chapel Hill
Chapel Hill, North Carolina 27599

Summary

Background: The regulated assembly of microtubules is essential for bipolar spindle formation. Depending on cell type, microtubules nucleate through two different pathways: centrosome-driven or chromatin-driven. The chromatin-driven pathway dominates in cells lacking centrosomes.
Results: Human RHAMM (receptor for hyaluronic-acid-mediated motility) was originally implicated in hyaluronic-acid-induced motility but has since been shown to associate with centrosomes and play a role in astral spindle pole integrity in mitotic systems. We have identified the *Xenopus* ortholog of human RHAMM as a microtubule-associated protein that plays a role in focusing spindle poles and is essential for efficient microtubule nucleation during spindle assembly without centrosomes. XRHAMM associates both with γ-TuRC, a complex required for microtubule nucleation and with TPX2, a protein required for microtubule nucleation and spindle pole organization.
Conclusions: XRHAMM facilitates Ran-dependent, chromatin-driven nucleation in a process that may require coordinate activation of TPX2 and γ-TuRC.

Introduction

Eukaryotic chromosome segregation during both mitosis and meiosis relies on the capacity of cells to organize polymeric tubulin into bipolar spindles. The mechanistic details of microtubule nucleation during spindle assembly varies among cell types; it depends primarily on whether preassembled microtubule organizing centers (MTOCs) are present. In most somatic cells, spindle assembly occurs via an MTOC-directed pathway where microtubules nucleate from a pair of separating centrosomes [1, 2]. In many germ line cells, spindle assembly occurs without centrosomes (anastral spindles) through a pathway driven by chromatin nucleation of microtubules [3, 4]. Thus, germ line cells have mechanisms to nucleate microtubules without the presence of a preassembled MTOC.

*Correspondence: aaron_groen@students.hms.harvard.edu

Although microtubule nucleation from centrosomes is well understood, nucleation without centrosomes remains ill defined [5]. Anastral microtubule nucleation is driven by chromatin and is thought to involve the small GTP binding protein Ran [6]. When Ran is bound to GTP, it induces the assembly of microtubules by releasing and activating various spindle components, such as nuclear mitotic apparatus (NuMA) and TPX2, from importin α/β complexes [7]. Because Ran guanine nucleotide exchange factor (RCC1) localizes to chromatin, whereas the cytosol contains Ran GTPase activating protein (GAP), GTP bound Ran is restricted to a region near chromatin, thereby concentrating microtubule nucleation near chromatin [8]. The nucleation factor(s) triggered by Ran is not well defined. Previous studies show that the RanGTP-driven assembly of microtubules is dependent on the γ-tubulin ring complex (γ-TuRC), a known microtubule nucleator [6], and TPX2, which may also nucleate microtubules [9]. How TPX2 and γ-TuRC precisely function to induce microtubule nucleation is not well understood [6].

Once microtubules assemble near chromatin, a combination of plus-end-directed and minus-end-directed microtubule-based motor proteins are thought to arrange the microtubules into a bipolar spindle with two focused poles [10]. These anastral poles accumulate NuMA and TPX2, both of which are thought to participate in assembly of protein complexes that stabilize spindle poles [11]. It is not known whether other factors are involved in focusing spindle poles. Through analysis of the spindle pole *Xenopus* microtubule associated protein (MAP), XRHAMM, we present evidence that a new factor contributes to chromatin-dependent microtubule nucleation and the focusing of anastral spindle poles.

Results and Discussion

Identification of XRHAMM from *Xenopus* Egg Extracts

Taxol-stabilized GMPCPP microtubules were incubated with clarified metaphase-arrested *Xenopus* egg extract at 0°C to identify MAPs that function during spindle assembly. The proteins were isolated by two rounds of centrifugation through sucrose cushions and eluted with high salt [12]. A ~150 kDa protein, designated XMAP150, was identified by ion trap mass spectrometry (Figure 1A; courtesy of W. Lane). The full-length polypeptide is composed of 1175 amino acids that have a high probability of assembling into coiled coils (accession number AY729653) [13].

Database searches revealed that XMAP150 is homologous to murine and human RHAMM/IHABP (receptor for hyaluronic-acid-mediated motility/intracellular hyaluronic acid binding protein); therefore, we will refer to it as XRHAMM. The *Xenopus*, mouse, and human proteins are particularly homologous at their N and C termini, where XRHAMM is ~45% and ~65% identical to human and mouse RHAMM/IHABP, respectively (Figure

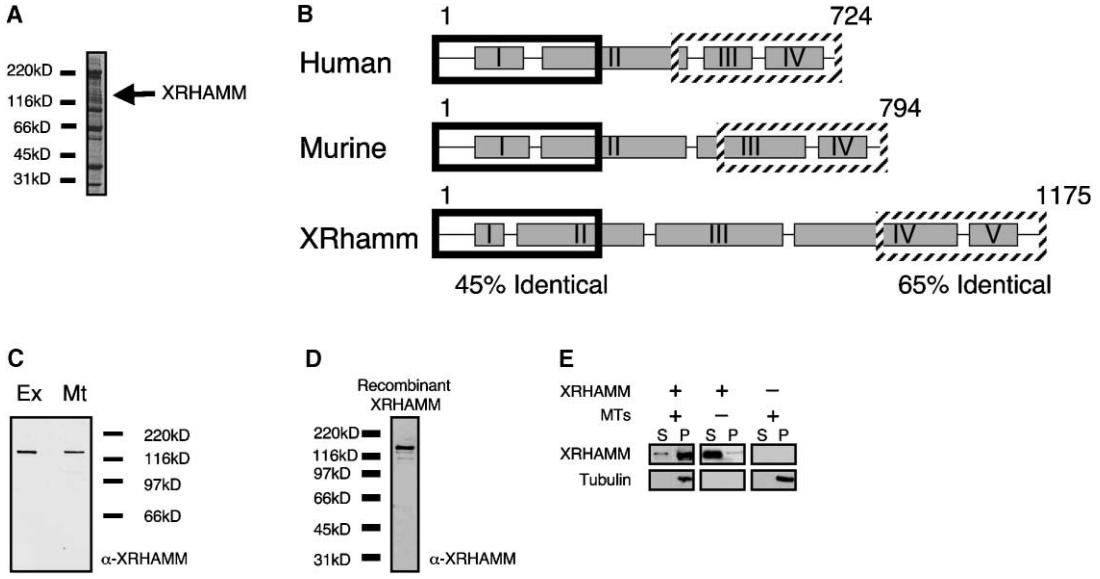

Figure 1. Identification of XRHAMM

(A) The Coomasie-stained SDS-PAGE gel of proteins binding to GMPCPP-polymerized microtubules from meiotic *Xenopus* egg extracts.
(B) Protein sequence alignment of *Xenopus* (XRHAMM), human, and murine RHAMM; the most homologous regions contained at the N and C termini are highlighted. Domains I–IV for mouse and human and I–V for *Xenopus* indicate predicted coiled coil regions.
(C and D) Specificity of XRHAMM antibodies. In (C), XRHAMM immunoblots of meiotic *Xenopus* extract (Ex) and the proteins binding to polymerized microtubules (Mt) from *Xenopus* extract are shown. In (D), An XRHAMM immunoblot of the purified recombinant protein expressed in SF9 insect cells is shown.
(E) XRHAMM-microtubule copelleting assays. Supernatant (S) and pellet (P) of XRHAMM and polymerized microtubules (MTs), XRHAMM alone, or microtubules alone are shown.

1B; [14, 15]). As suggested by its name, RHAMM/IHABP was originally implicated in hyaluronic-acid-induced motility but has since been shown to associate with centrosomes and play a role in astral spindle pole integrity in mitotic systems [16, 17].

Polyclonal antibodies were raised against XRHAMM's C-terminal 137 amino acids and affinity purified to study the function of XRHAMM. Immunoblotting of *Xenopus* egg extracts (meiotic and interphase), our MAP preparation, and recombinant XRHAMM with affinity purified anti-XRHAMM antibodies detects a single comigrating polypeptide of the molecular weight predicted for XRHAMM, demonstrating antibody specificity (Figures 1C and 1D; data not shown). Recombinant XRHAMM copellets with taxol-stabilized GMPCPP microtubules, demonstrating that XRHAMM is a microtubule-associated protein (Figure 1E).

XRHAMM Localizes to Spindle Poles in a Dynein-Dependent Manner

To help understand the function of XRHAMM, we examined its localization by indirect immunofluorescence of *Xenopus* tissue culture (XTC) cells (Figure 2A). XRHAMM localizes to spindle microtubules with appreciable concentration at the two spindle poles. XRHAMM immunostaining was not observed on spindle midzone microtubules during anaphase A and became undetectable during telophase. During interphase, XRHAMM could also be detected on centrosomes; this was determined by costaining with the centriolar protein centrin (Figure 2A, bottom row).

Examination of XRHAMM localization on spindles formed with *Xenopus* egg extracts revealed a similar distribution to that observed in intact cells. XRHAMM was enriched at the spindle poles and showed diffuse localization on all spindle microtubules (Figure 2B).

The microtubule minus-end-directed motor complex, dynein/dynactin, is thought to have a role in focusing the minus ends of microtubules into a pole by transporting various structural factors, such as TPX2 and NuMA, to the minus ends [15, 18]. We therefore tested whether XRHAMM spindle pole localization requires the function of the dynein/dynactin complex. We blocked dynein/dynactin activity during spindle assembly in *Xenopus* extracts with 1 mg/ml of the dynactin complex component p50, a dominant-negative treatment that produces splayed spindle poles [18], and then analyzed XRHAMM localization by immunofluorescence and linescans (Figures 3A and 3B). Under such conditions, XRHAMM failed to localize to the ends of the unfocused spindle poles and instead showed a uniform distribution on spindle microtubules (Figure 3). We also found that XRHAMM immunoprecipitates contain the dynactin component p50 but not dynein intermediate chain 70.1, showing that a physical interaction exists between XRHAMM and the dynactin complex (data not shown; [19, 20]). Thus, XRHAMM most likely requires the activity of the dynein/dynactin complex for localization or maintenance of localization on the microtubule minus ends of the spindle pole.

XRHAMM Facilitates Anastral Spindle Assembly

To probe the function of XRHAMM in spindle assembly, we performed immunodepletion experiments. These

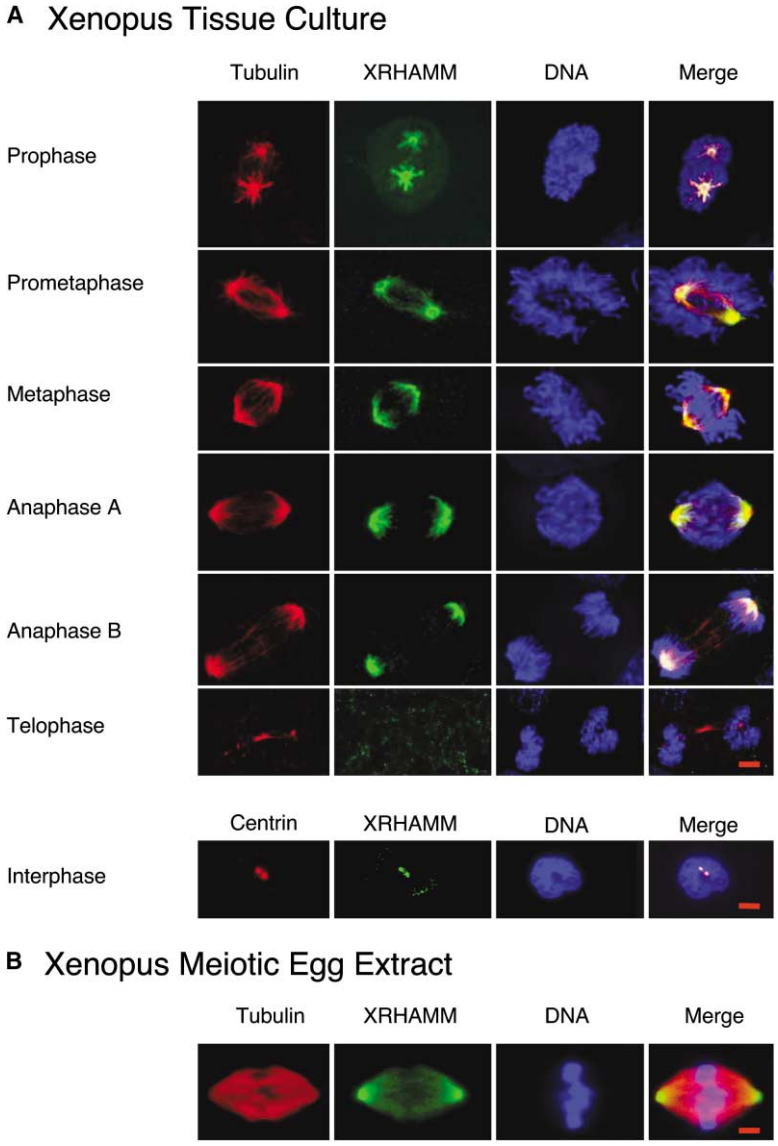

Figure 2. XRHAMM Concentrates at Spindle Poles

(A) The localizations of XRHAMM (green), tubulin (red), and DNA (blue) throughout the cell cycle in *Xenopus* XTC tissue cells. XRHAMM associates with microtubules during prophase and metaphase, with higher concentrations near the spindle pole. During anaphase, XRHAMM is undetectable in the spindle midzone, but during telophase, it is not on the mitotic spindle. During interphase, XRHAMM concentrates as puncta that colocalize with the centriole marker centrin, indicating that it localizes to the centrosome.

(B) The localization of XRHAMM in *Xenopus* egg extract spindles. XRHAMM localizes to the microtubules of the spindle and focuses at the spindle pole. The scale bar represents 3 μm.

were problematic with demembranated sperm nuclei (or sperm spindles) for triggering spindle assembly because sperm centrosomes contain significant amounts of XRHAMM (data not shown). Thus, we turned to anastral spindles assembled around DNA beads [21]. As in the case of sperm spindles, XRHAMM localized to the poles of anastral spindles (Figure 4A). Therefore, we can use spindles assembled on DNA beads as an alternative to test XRHAMM function by immunodepletion.

XRHAMM-depleted extracts did not assemble spindles efficiently (Figures 4A and 4B). Strikingly, no microtubule polymerization was detected around approximately 60% of the DNA beads. In contrast, mock-depleted extracts efficiently assembled bipolar spindles around 60% of the DNA beads (Figures 4A and 4B). Furthermore, addback of purified recombinant XRHAMM to endogenous levels (~70 nM) rescued spindle assembly defects to about 70% of mock-depleted extracts, suggesting that XRHAMM is at least partially responsible for the defects (Figures 4A–4C). The incomplete rescue may result from either the recombinant protein not being completely functional or codepleting factors also being responsible for the defects. Thus, XRHAMM and, possibly, codepleting factors are essential for efficient anastral spindle assembly in *Xenopus* egg extract.

Given that depletion of XRHAMM blocks microtubule assembly in anastral spindles, we assessed the possibility that XRHAMM functions downstream of Ran in chromatin-driven spindle assembly. Microtubule assembly can be induced by adding a constitutively active mutant of Ran, Ran(Q69L)-GTP (which is unable to hydrolyze GTP) to extract [6, 22]. The assembled microtubules form anastral poles. Extracts depleted of XRHAMM form approximately 80% fewer anastral poles than mock depleted extracts do, suggesting that XRHAMM plays a role in efficient Ran-dependent microtubule assembly (Figure 4D). The quantification of pelleted Ran-induced microtubules isolated from extracts with and without XRHAMM confirmed that counting asters accurately reflected the associated microtubule assembly defects (data not shown). The addition of recombinant XRHAMM to depleted extracts rescued aster assembly defects to

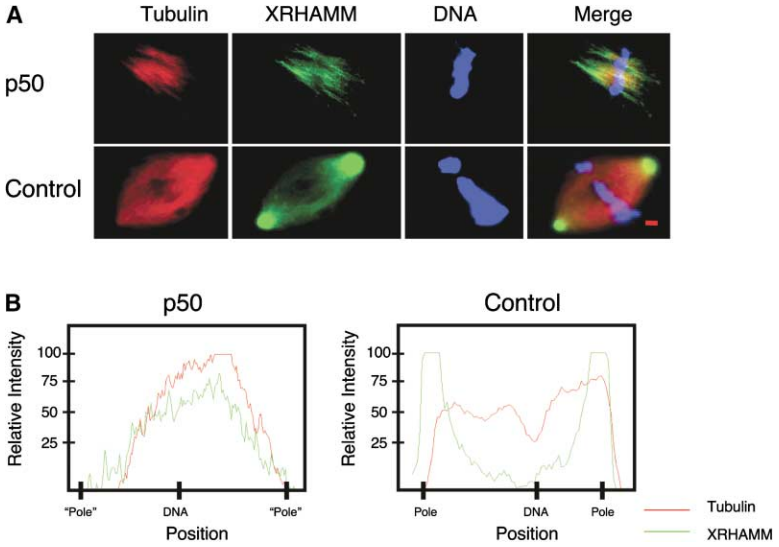

Figure 3. XRHAMM Depends on Dynein/Dynactin Complex to Concentrate on Spindle Poles

(A) Unlike in control spindle reactions, XRHAMM is not concentrated on the unfocused spindle pole when dynein/dynactin function has been perturbed with 1 mg/ml of p50.

(B) Linescans of p50 treated (left) and control spindles (right) stained for XRHAMM (green) and tubulin (red). Notice that the fluorescence intensity of XRHAMM at the pole is higher relative to the midzone only when the dynein/dynactin complex is active. The scale bar represents 2 μm.

approximately 60% of mock-depleted extracts, demonstrating that XRHAMM and, possibly, codepleting factors have a role in the Ran-dependent assembly of microtubules (Figure 4D). Thus, XRHAMM plays a role in microtubule nucleation or stabilization by the chromatin pathway in *Xenopus* egg extracts.

XRHAMM Associates with TPX2 and γ-Tubulin

To help understand how XRHAMM affects microtubule assembly, we isolated XRHAMM interacting proteins by immunoprecipitation from *Xenopus* extracts. XRHAMM immunoprecipitates contain ~90% of the endogenous XRHAMM contained in extract but do not contain stoichiometric binding proteins when analyzed by Coomassie-stained protein gel electrophoresis (PAGE) (data not shown; Figure 5A). However, immunoblots show that XRHAMM interacts with TPX2 and γ-TuRC component γ-tubulin (Figure 5B; [23]). The immunoprecipitates also contain the γ-TuRC component XGRIP109, suggesting that XRHAMM interacts with γ-TuRC (data not shown; [24]).

To verify the XRHAMM and TPX2 interaction, we performed immunoprecipitations from *Xenopus* extracts with TPX2 antibodies. However, we were unable to detect an interaction, possibly suggesting that the antibodies perturb the interaction. Therefore, we performed pull-downs from *Xenopus* extracts with either GST or GST fused to full-length TPX2. By immunoblotting, XRHAMM was specifically retrieved with GST-TPX2 but not GST alone (Figure 5C). We were also unable to demonstrate direct binding of TPX2 and XRHAMM through the use of recombinant proteins, indicating that additional factors may stabilize the interaction in extracts (data not shown).

To verify the XRHAMM and γ-tubulin interaction, we performed immunoprecipitations with affinity purified γ-tubulin antibodies. By immunoblotting, we were able to detect XGRIP109, suggesting that γ-TuRC was present in our immunoprecipitations, but we were unable to detect a specific interaction between γ-tubulin and XRHAMM (data not shown). Thus, γ-tubulin antibodies may not detect the interaction.

XRHAMM may make microtubule nucleation more efficient by linking together proteins that are essential for chromatin-dependent microtubule nucleation. XRHAMM immunoprecipitations in either TPX2- or γ-tubulin-depleted extracts each contain TPX2 or γ-tubulin, respectively (data not shown), showing that the XRHAMM-γ-tubulin interaction is independent of TPX2 and that the XRHAMM-TPX2 interaction is independent of γ-tubulin. We also could not detect an interaction between TPX2 and γ-tubulin (by immunoprecipitation with either TPX2 or γ-tubulin affinity purified antibodies), suggesting that either the interaction is weak and only occurs through a substoichiometric association with XRHAMM or our antibodies perturb the interaction (data not shown). Thus, TPX2 and γ-tubulin may not directly interact, and XRHAMM may link together a microtubule nucleation complex containing TPX2 and γ-TuRC.

XRHAMM Colocalizes with TPX2 and γ-Tubulin at the Spindle Pole

We find that XRHAMM colocalizes with TPX2 and γ-tubulin at the spindle pole by indirect immunofluorescence microscopy of fixed extract spindles (data not shown); this is consistent with the association of TPX2 and XRHAMM and the detection of γ-tubulin in XRHAMM immunoprecipitates. To examine the localization of TPX2, γ-tubulin, and XRHAMM in unfixed samples, we imaged extract spindles with XRHAMM and TPX2 or XRHAMM and γ-tubulin directly labeled antibodies. It was evident that XRHAMM/TPX2 (Figure 5D) and XRHAMM/γ-tubulin (Figure 5E) colocalized at spindle poles; however, neither precisely colocalized throughout the length of the spindle. We observed that XRHAMM localized as puncta that were not always precisely coincident with either TPX2 (Figure 5D) or γ-tubulin (Figure 5E). These experiments suggest that XRHAMM associates with TPX2 and γ-tubulin primarily at spindle poles and that these proteins may have other nonoverlapping functions throughout the spindle.

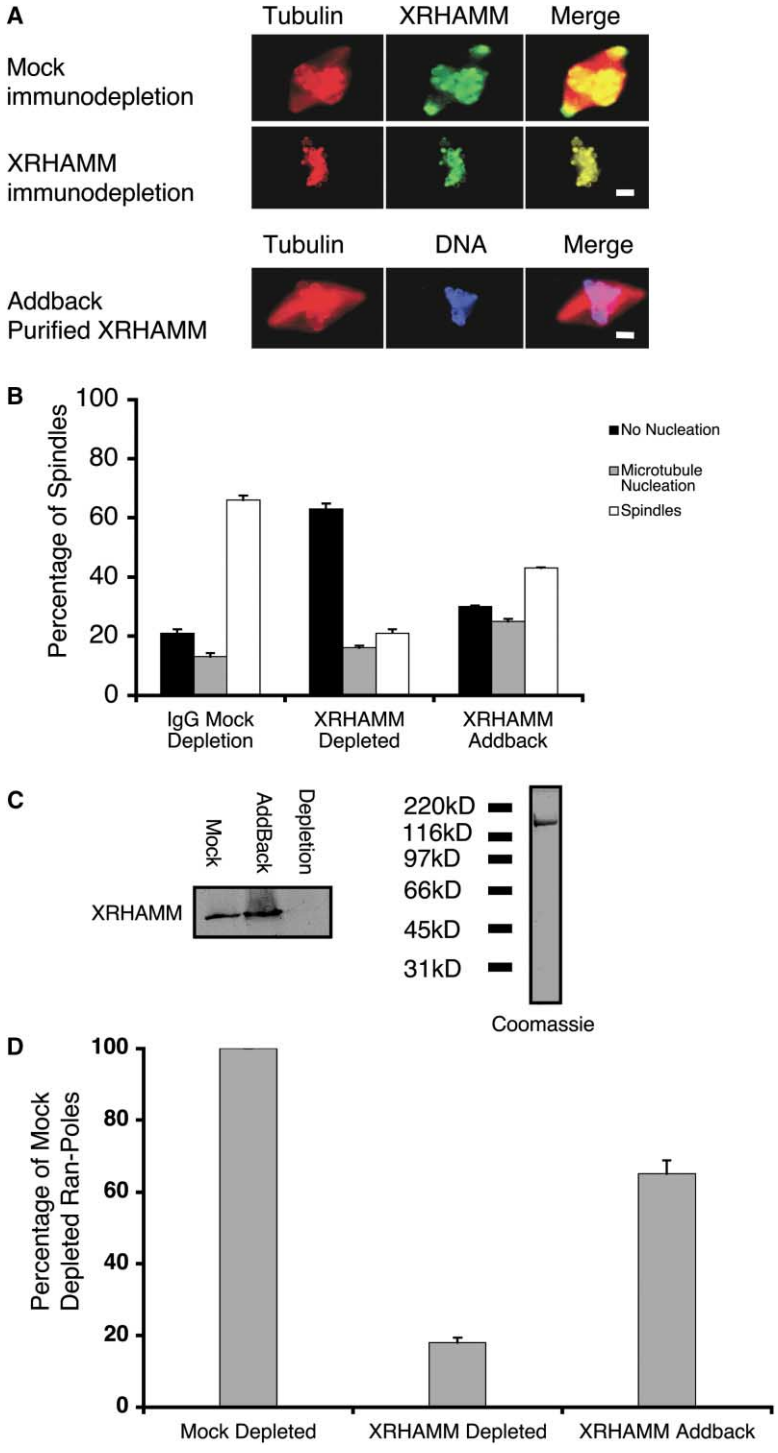

Figure 4. XRHAMM Is Essential for Efficient Anastral Spindle Assembly

(A) Anastral DNA bead spindles formed in extracts mock depleted, XRHAMM depleted, and XRHAMM depleted with recombinant XRHAMM added back to endogenous levels (70 nM). Note that without XRHAMM, no nucleation occurs around the DNA beads. The scale bar represents 3 μm.

(B) Quantification of phenotypes associated with XRHAMM depletions (number of experiments: 3; number of counted structures: 900; error bars = standard error of the mean). DNA bead spindles efficiently assembled around groups of approximately 15–40 beads, and thus any bead aggregates of this size that did not assemble spindles or microtubules were counted as no nucleation. Note that the dominant phenotype of XRHAMM-depleted extracts is DNA bead aggregates that do not nucleate microtubules, whereas spindles are the dominant phenotypes in mock depletions or depleted extracts rescued with purified recombinant XRHAMM.

(C) (Left) XRHAMM immunoblot of extracts mock depleted, depleted with XRHAMM addback to endogenous levels (70 nM), and depleted for XRHAMM. (Right) Coomassie-stained SDS-PAGE gel of purified recombinant XRHAMM.

(D) Quantification of the number of Ran(Q69L)GTP-anastral poles (added at 0.3 mg/ml) formed in mock-depleted extracts, XRHAMM-depleted extracts, and XRHAMM-added-back-to-XRHAMM-depleted extracts. Note that without XRHAMM, fewer Ran dependent spindle poles assemble (number of experiments = 3; error bars = standard error of the mean).

XRHAMM Is Required for Concentrating TPX2 on Spindle Poles

We observed that TPX2, γ-tubulin, and XRHAMM colocalize at the spindle poles of both centrosomal and anastral spindles (Figure 4B, data not shown). To test whether the localization of TPX2 and γ-tubulin depended on XRHAMM, we compared the ability of extracts to localize TPX2 and γ-tubulin on dimethyl-sulfoxide (DMSO)-induced microtubule spindle poles in the presence or absence of XRHAMM. DMSO induces microtubule assembly without centrosomes and, thus, allows the analysis of spindle pole assembly in XRHAMM-depleted extracts defective in efficient microtubule assembly. Similar to the poles formed in DNA bead spindles, DMSO asters localized XRHAMM at the foci (Figure 6A). These localizations confirmed our observation that XRHAMM localized to polymerized microtubules in extract independent of centrosomes and

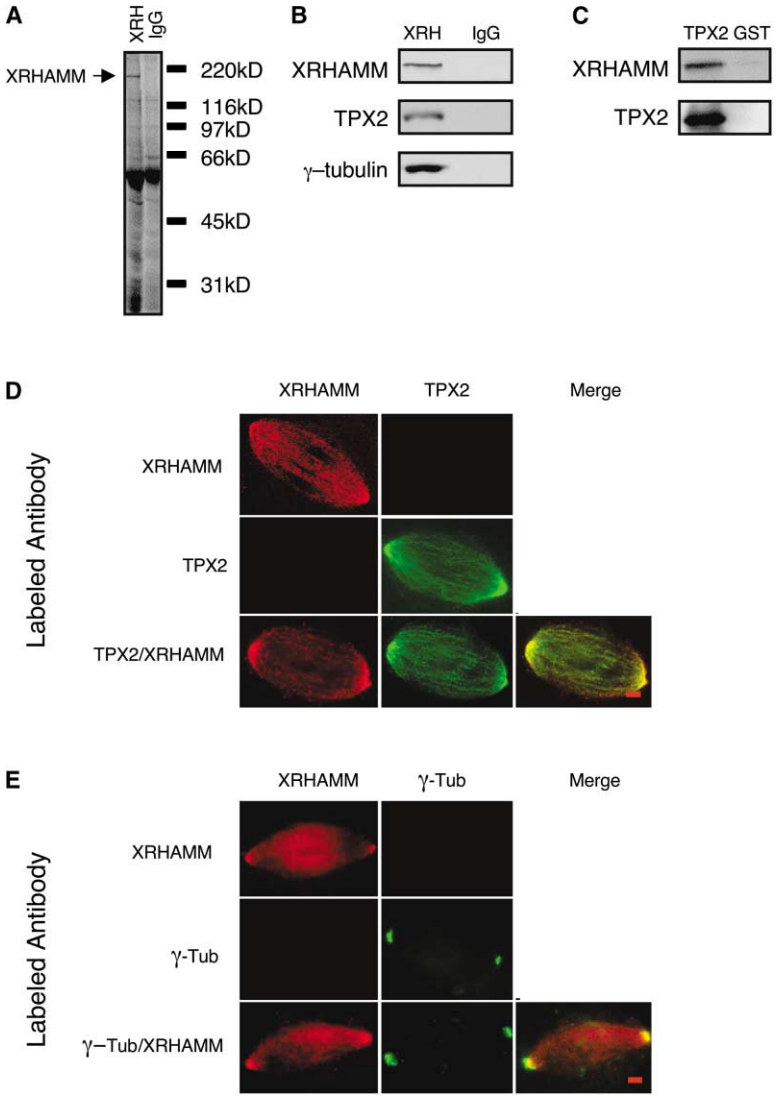

Figure 5. XRHAMM Interacts with TPX2 and γ-tubulin

(A) Coomassie-stained SDS-PAGE of lysates of XRHAMM and IgG immunoprecipitations. Note the lack of specific stoichiometric XRHAMM-interacting proteins.

(B) Immunoblots showing XRHAMM immunoprecipitates with TPX2 and γ-tubulin from meiotic *Xenopus* extracts.

(C) Immunoblots showing that GST-TPX2 specifically interacts with XRHAMM.

(D) The localizations of XRHAMM and TPX2 on unfixed *Xenopus* egg extract spindles. Note that XRHAMM and TPX2 colocalize predominantly at the spindle pole.

(E) The localizations of XRHAMM and γ-tubulin on unfixed *Xenopus* egg extract spindles. Note that XRHAMM and γ-tubulin only colocalize at the spindle pole. The scale bar represents 2 μm.

showed that DMSO asters are a comparable model for our experiment.

The anastral DMSO-induced spindle poles assembled in XRHAMM-depleted extracts were unfocused compared to controls (Figure 6B, top and middle rows), yet TPX2 and γ-tubulin remain localized to the XRHAMM-deficient poles (Figure 6B, middle row, and Figure 6C, bottom row). Thus, XRHAMM is not essential for TPX2 and γ-tubulin to bind to microtubules. However, in contrast to the case of mock-depleted extracts (Figure 6B, top row), TPX2 did not concentrate on the centers of the poles assembled in XRHAMM-depleted extracts but instead localized all over the microtubule structures (Figure 6B, middle row). Interestingly, unlike TPX2, γ-tubulin localized to the centers of the XRHAMM-deficient spindle poles (Figure 6C, bottom row). The addition of purified recombinant XRHAMM rescued not only the unfocused poles of the XRHAMM-deficient structures, but also the mislocalization of TPX2, demonstrating that these defects are due entirely to the removal of XRHAMM (Figure 6B, bottom row).

The localization of γ-tubulin on XRHAMM-deficient spindle poles was more diffuse than the localization on mock-depleted controls (Figure 6C). Similar to γ-tubulin, NuMA and the dynein/dynactin complex were diffusely localized near the centers of the XRHAMM-deficient aster structures (Figure 6C; data not shown). However, we cannot determine whether these changes in localization result from, or contribute to, the unfocused spindle poles assembled in XRHAMM depleted extracts. These localizations do indicate that XRHAMM is not required for the dynein/dynactin-dependent arrangement of microtubules in a spindle pole structure [25] but rather plays a role in focusing poles, possibly through the activity of TPX2.

XRHAMM-Associated Proteins Nucleate Microtubules in Pure Tubulin Solutions

We found that XRHAMM plays a role in chromatin-induced microtubule nucleation in *Xenopus* egg extracts. To test whether XRHAMM directly induces microtubule assembly in vitro, we mixed recombinant XRHAMM with pure tubulin. We found that XRHAMM did not detectably nucleate microtubules in vitro but

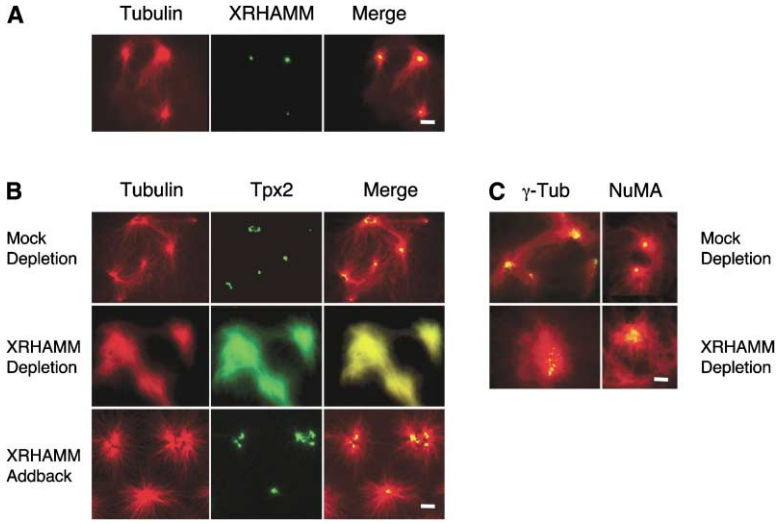

Figure 6. XRHAMM Is Essential for Concentrating TPX2 on Spindle Poles

(A) DMSO-induced microtubule spindle poles concentrate XRHAMM at the pole. The scale bar represents 3 μm.

(B and C) DMSO-induced microtubule poles assembled in XRHAMM-depleted extracts are not focused and do not concentrate TPX2 at the pole, whereas NuMA and γ-tubulin remain faintly localized to the unfocused center of the pole. NuMA and γ-tubulin were sometimes difficult to image on the unfocused spindle poles because the distribution was dispersed and faint. The images shown in this figure are representative for the bright distributions that were observed in many of the poles examined (>60%). Addition of purified recombinant XRHAMM rescues the unfocused pole defect and the mislocalization of TPX2. The scale bar represents 3 μm.

could strongly associate and bundle polymerized microtubules (data not shown). Thus, XRHAMM indirectly contributes to microtubule nucleation.

We next tested whether XRHAMM plus associated proteins could nucleate microtubules by adding magnetic beads coated with anti-XRHAMM to *Xenopus* extract. As expected, XRHAMM beads associate with TPX2 and γ-TuRC (data not shown). However, we did not observe microtubule assembly (data not shown; Figure $7A_i$). To test whether the protein complexes recruited to these beads were able to nucleate microtubules in vitro without the presence of various catastrophe factors present in extract, we washed the beads and challenged them with pure tubulin below the critical concentration of self-assembly (1 mg/ml). Once again, we did not observe microtubule assembly (Figure $7A_{ii}$).

We next tested whether Ran(Q69L)-GTP could induce microtubule assembly from XRHAMM beads. When XRHAMM beads were placed in extract treated with Ran(Q69L)-GTP, microtubules assembled around the beads (Figure $7A_{iii}$). Experiments in extract cannot distinguish microtubule nucleation versus stabilization; therefore, we washed and incubated the beads in pure tubulin solutions (1 mg/ml). XRHAMM beads were added to Ran(Q69L)GTP-treated extract plus nocodazole to suppress microtubule polymerization and were incubated for 20–30 min (Figure $7A_{iv}$). The beads were then retrieved, washed at 4°C (to ensure complete microtubule depolymerization), and challenged with pure tubulin (1 mg/ml). Remarkably, these beads nucleated abundant microtubules in vitro (Figure $7A_v$). Interestingly, microtubule assembly was not detected when TPX2 or γ-tubulin bound antibody beads were incubated in Ran(Q69L)-GTP-treated extract (data not shown), possibly suggesting that the TPX2 or γ-tubulin antibodies may perturb the function of the nucleation complex.

Because TPX2 associates with XRHAMM and has been implicated in microtubule nucleation, we tested whether microtubule nucleation from XRHAMM beads was TPX2-dependent [9]. XRHAMM beads isolated from Ran(Q69L)GTP and nocodazole-treated extracts immunodepleted for TPX2 (approximately 80% depleted; Figure 7C) contain XRHAMM and γ-tubulin but were unable to nucleate microtubules in pure tubulin solutions under any condition (Figure $7B_{ii}$; data not shown). Addition of recombinant TPX2 to the extract could rescue this defect. Addition of TPX2 to beads after removal from TPX2-depleted extract, however, could not rescue this defect (data not shown). Thus, TPX2 is essential for microtubule nucleation from XRHAMM beads, both in extracts and with pure tubulin, but the TPX2 must be present in extract perhaps to promote assembly of nucleation complexes.

We also tested if nucleation from XRHAMM beads was dependent on γ-TuRC, an XRHAMM-associated protein complex that has an established role in microtubule nucleation [26]. XRHAMM beads isolated from Ran(Q69L)-GTP and nocodazole-treated extracts immunodepleted of γ-tubulin (approximately 80%–90% depleted), an essential component of the γ-TuRC [25], contain XRHAMM and TPX2 but were unable to nucleate microtubules in pure tubulin solutions (Figures $7B_{iii}$ and 7C; data not shown). We have so far been unable to purify enough functional γ-tubulin to complement the depleted extract. Thus, similar to microtubule assembly around chromatin, microtubule nucleation by X-RHAMM beads is dependent on RanGTP, TPX2, and γ-tubulin.

Conclusions

In this study, we identify XRHAMM, the *Xenopus* ortholog of human RHAMM/IHABP. Previously, RHAMM/IHABP was thought to have intracellular and extracellular functions involving the glycosaminoglycan hyaluronan, but recent studies have demonstrated that RHAMM/IHABP colocalizes with microtubules and is important for maintaining spindle pole stability, suggesting that RHAMM/IHABP function instead involves the microtubule cytoskeleton [15]. Consistent with this idea was our identification of XRHAMM as one of the predominant MAPs in meiotic *Xenopus* egg extracts; we showed that it not only associates with proteins established in microtubule nucleation but is essential for efficient anastral spindle assembly. Our data show that XRHAMM has two functions: to help to focus the anastral pole and

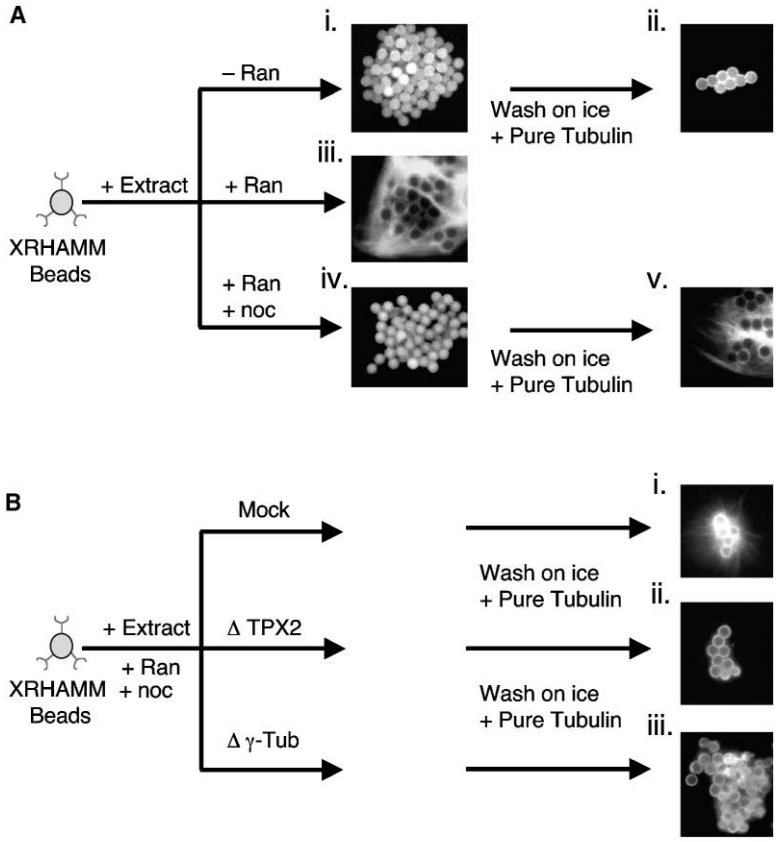

Figure 7. XRHAMM-Associated Proteins Nucleate Microtubules in Pure Tubulin Solutions

(A) Protein A beads bound to XRHAMM antibodies and treated with Ran(Q69L)GTP-activated extracts can assemble microtubules (iii). Beads retrieved from Ran(Q69L)GTP-treated extract in the presence of nocodazole (noc; iv), washed on ice with CSF-XB, and challenged with pure tubulin at 1 mg/ml at 37°C can nucleate microtubules (v). Ran(Q69L)GTP is required to induce microtubule nucleation in vitro (ii), showing that XRHAMM-associated proteins do not merely stabilize microtubules.

(B) Depletion of either TPX2 (ii) or γ-tubulin (iii) inhibits nucleation from XRHAMM beads in pure tubulin solutions (1 mg/ml).

(C) Immunoblots showing depletions of TPX2 and γ-tubulin in extracts used in (B). Notice that XRHAMM does not significantly codeplete with TPX2 or γ-tubulin.

to help nucleate microtubules by the Ran-dependent chromatin-driven pathway. Both of these functions depend on interactions with TPX2. The nucleation function of XRHAMM also depends on the interaction with γ-tubulin.

XRHAMM Is Required for Pole Focusing

An anastral spindle pole assembles with the microtubule minus ends concentrated at its center [27]. Anastral spindle pole assembly is thought to involve the activities of various MAPs and plus-end- and minus-end-directed motor proteins [28]. The activities of the motor proteins and MAPs that concentrate at the pole focus the minus ends of microtubules into a spindle pole [27]. Evidence suggests that MAPs concentrate on the spindle pole either by directly associating with the minus ends of microtubules, as in the case of γ-TuRC, or by being delivered to the minus ends through the microtubule minus end motor activity of dynein, as in the case of NuMA or TPX2 [25]. Through either the inhibition of dynein or the microtubule-associated proteins, a focused spindle pole can become disrupted [18].

XRHAMM and TPX2 depend on the dynein/dynactin complex to perform the functions of focusing spindle poles (Figure 3) [11]. However, XRHAMM is not required for the dynein/dynactin-dependent arrangement of the minus ends of the microtubules into a spindle pole because NuMA, the dynein/dynactin complex, and γ-tubulin remain at the centers of the unfocused spindle poles assembled in XRHAMM-depleted extracts (Figure 6) [25, 29, 30]. Thus, XRHAMM plays either a direct or indirect role (possibly through TPX2) in focusing the minus ends of the microtubules either parallel to or after dynein/dynactin.

XRHAMM Enhances Ran-GTP-Dependent Microtubule Assembly

Ran-dependent microtubule assembly is essential for the chromatin-driven spindle assembly observed in anastral spindles [31]. We find XRHAMM is not essential for Ran-dependent microtubule assembly because Ran(Q69L)GTP induces microtubule assembly in XRHAMM-depleted extracts (Figure 4D). We also find that the addition of ~4× the endogenous concentration of TPX2 (~400 nM) to XRHAMM-depleted extracts also rescues microtubule assembly defects (data not shown). Thus, XRHAMM is clearly not essential for Ran-dependent microtubule assembly and may enhance the activi-

ties of XRHAMM-interacting proteins such as TPX2, making microtubule nucleation more efficient in *Xenopus* egg extracts.

How Does Chromatin-Driven Microtubule Nucleation Occur?

The pathway of chromatin-induced microtubule nucleation during anastral spindle assembly is not well defined. One problem is that experiments in extracts or in vivo cannot clearly distinguish microtubule nucleation from microtubule stabilization. The two are typically scored together as "microtubule assembly." Because cells and extracts contain multiple microtubule stabilizing and destabilizing factors, this distinction can only be made with pure tubulin. Our assay with XRHAMM beads is the first assay in which the Ran-dependent microtubule nucleation pathway has been observed in pure tubulin solutions (Figure 7).

We find that Ran-dependent microtubule nucleation in pure tubulin solutions depends on both TPX2 and γ-tubulin. Although the γ-TuRC, which contains γ-tubulin, has an established role in microtubule nucleation, it is not clear how TPX2 precisely functions in this process. TPX2 is essential for the Ran-dependent activation of Aurora A kinase, yet it is not known whether this active kinase has a role in microtubule assembly [32]. We found that Aurora kinase inhibitors [33] did not inhibit Ran-dependent microtubule nucleation (from XRHAMM beads in pure tubulin solutions or in extract), suggesting that Aurora A kinase plays no role in Ran-dependent microtubule assembly. Recombinant TPX2 can nucleate microtubules in vitro, showing that TPX2 may play a central role in the mechanism of microtubule nucleation [9], though the additional requirement of γ-tubulin for microtubule nucleation in extract suggests that the mechanism is more complex.

Although the XRHAMM bead assay reported here is a step forward, the precise roles of Ran, TPX2, γ-tubulin, and XRHAMM in nucleation are not yet understood. Microtubule nucleation depends on the presence of Ran-GTP in the extract, but so far we have detected no difference in the protein composition of XRHAMM beads retrieved from Ran-GTP and control extracts. The two proteins we know are essential for nucleation, γ-tubulin and TPX2, are recruited to similar levels in both cases. We also find that the addition of importin α/β, a complex that binds to and sequesters the activities of TPX2, inhibits in vitro microtubule nucleation from XRHAMM beads (data not shown), suggesting that the importins have a role in regulating the nucleation complex. However, because the importins did not coimmunoprecipitate with XRHAMM (as analyzed by immunoblots), we suspect that either our antibodies perturb the interaction or the importins may regulate an unidentified factor (data not shown). We suppose that undetermined proteins are required in addition to TPX2 and γ-tubulin and/or that one or more must be posttranslationally modified. In future experiments, we will use pure proteins to reconstitute microtubule nucleation testing models in which TPX2 may activate γ-TuRC for nucleation.

Experimental Procedures

Identification of XRHAMM

Identification of binding proteins to taxol-stabilized GMPCPP-polymerized microtubules in *Xenopus* meiotic extracts was described previously [12]. Proteins were identified by liquid chromatography-mass spectrometry/mass spectrometry (LC-MS/MS) as described [12].

XRHAMM-Microtubule Copelleting Assay

Approximately 1 μM of taxol-stabilized GMPCPP-polymerized microtubules (±5 μg of XRHAMM, bound on ice for 5 min) was spun through BRB80/30% glycerol cushion at 227,000 × g. Samples were diluted in sample buffer and analyzed by immunoblots.

Xenopus Extract

Metaphase-arrested *Xenopus* extract (CSF), X-rhodamine-labeled tubulin, demembranated sperm nuclei, and extract spindles were prepared as described previously [34–36]. Cycled meiotic spindles assembled from sperm nuclei were formed as previously described [34]. Anastral DNA bead spindles were formed as detailed previously [21].

XRHAMM-, TPX2-, and γ-tubulin-immunodepleted CSF was made by three rounds of incubating 50 μl of ProteinA dynabeads (Dynal) bound to 20 μg of affinity purified XRHAMM polyclonal antibodies with 150 μl of extract for 1 hr at 4°C. Immunoblots were used to confirm depletions.

Microtubule Pole Formation in *Xenopus* Extract

DMSO microtubule poles were formed with the addition of 5% DMSO and were imaged 20 min later with directly labeled tubulin (70 μg/ml), directly labeled TPX2, γ-tubulin, and NuMA antibodies (10–50 μg/ml). RanGTP poles were induced by the addition of Ran(Q69L)GTP to 0.3 mg/ml and were imaged similarly [22, 37]. The number of Ran-induced poles was counted from each sample (mock-depleted, XRHAMM-depleted, and XRHAMM addback to XRHAMM-depleted extracts) per 2 μl of extract and was expressed as a percentage of mock-depleted poles for each experiment.

Immunofluorescence

TPX2 and XRHAMM colocalization on spindles was imaged in real time with spinning disk confocal microscopy. For details, see the Supplemental Data available with this article online. Images were acquired with a 100×/1.4 NA Plan Apochromat objective (Nikon) on a Nikon TE-300 inverted microscope fitted with a Yokogawa spinning disk confocal head (Perkin Elmer) and Orca ER cooled CCD camera set to 2 × 2 binning (Hamamatsu) with MetaMorph software (Universal Imaging) to capture the 488 and 568 wavelengths almost simultaneously, as previously described [38].

The localization of γ-tubulin, XRHAMM, NuMA, and the dynein/dynactin complex on spindles and DMSO-induced spindle poles were imaged on an upright Nikon E800 with a cooled CCD (Princeton Instruments) and MetaMorph software to control shutters, wavelength selection, and image acquisition with directly labeled γ-tubulin, TPX2, and NuMA antibodies (10–50 μg/ml) and directly labeled p50 (32 μg/ml).

XTC cells were fixed (and permeabilized at the same time) with 0.1% gluteraldehyde and 2% PFA in 200 mM KPIPES, 0.4% Triton, 20 mM KEGTA, and 2mM $MgCl_2$ and stained for immunofluorescence. Directly labeled antibodies were used at 1 μg/ml.

Construction of XRHAMM, TPX2, and Ran(Q69L) Plasmids

Xenopus TPX2 was amplified by PCR from a *Xenopus* ovary cDNA library (a kind gift from Aaron Straight, Stanford University) with the following primers: TPX_GEX_F (5′-CGCCCGGGGATGGAAGATACACAGGACACC-3′) and TPX_GEX_R (5′-CGGCGGCCGCTCAACACTTAAACCTGTCCGAGAAG-3′). The amplified DNA was digested with Sma1 and Not1 and inserted into the Sma1/Not1 sites of pGEX4T-1 (Amersham Biosciences). The construct pGST-TPX2 was created.

Oligos XRHAMM_5, 5′-AGTCATTGCCCAGTCAGC-3′) and XRHAMM_6 (5′-CAAACAAGTGGCGCACCC-3′, corresponding to nucleotides 3113–3130 of the XRHAMM coding sequence and a portion of the 3′-UTR, respectively, were used to PCR amplify a 430 base pair fragment of XRHAMM from the *Xenopus* ovary cDNA library and were used to screen the same library. The clone containing the largest insert was sequenced completely, and an SpeI site was introduced immediately upstream of the XRHAMM coding region by PCR to produce pSK(+)XRHAMM_SpeI. The XRHAMM coding region was excised from this plasmid with SpeI and li-

gated into the SpeI site of pFASTBAC HTc (Invitrogen), creating pFASTBAC_XRHAMM.

pMAL-Ran(Q69L)GTP (a kind gift from Adrian Salic) was subcloned into the BamH1 and Sal1 sites of pGEX4T-1.

Purification of Recombinant Ran(Q69L)GTP

GST-Ran(Q69L) was purified from BL21(DE3) (Stratagene) bacteria with conventional purification methods for GST agarose beads (Sigma). The purified protein was dialyzed in the following buffer: 10 mM HEPES, 200 mM KCl, and 1 mM GTP (pH 7.7). GST-TPX2 was purified according to the same protocol, except that GTP and EDTA were not included in the buffers.

Purification of Recombinant XRHAMM

pFASTBAC_XRHAMM was used to produce a baculovirus, as detailed in the Bac-to-Bac system (Invitrogen). His-XRHAMM was purified from SF9 cells (Invitrogen) with conventional purification methods. The purified protein was gel filtrated on a Superdex-200 column (Amersham Biosciences) equilibrated with 10 mM HEPES and 200 mM KCl (pH 7.7).

Purification of p50

p50 was purified as described previously [18].

Preparation of XRHAMM, Centrin, and γ-Tubulin Antibodies

The C-terminal 137 amino acids of XRHAMM were fused to the C terminus of GST, and the resulting fusion protein (GST-XRHAMM.C1) was purified from *E. coli* BL21DE3/pLysS cells with glutathione agarose (Sigma). *Xenopus* centrin, PCR amplified from the ovary cDNA library described above, was also expressed and purified from BL21DE3/pLysS as a GST fusion protein. GST-XRHAMM.C1 and GST-Xcentrin were used to immunize rabbits (Cocalico) and were affinity purified over Affi-Gel 10 (BioRad) columns covalently attached to the recombinant immunogens after depletion of α-GST antibodies from the sera.

γ-tubulin (Xen-C) C-terminal peptide antibodies were created as described previously [26, 39]. NuMA peptide antibodies were prepared as described previously [39].

Immunoprecipitations and Pull-Down Assays

Approximately 10 μg of XRHAMM antibodies (or rabbit IgG) were bound to 10 μl AffiPrep protein A beads (BioRad) and incubated with 150 μl of CSF for 1 hr at 4°C. Beads were washed six times with TBS and mixed with 15 μl of 2× sample buffer. Approximately 1 μl of each sample was run on SDS-PAGE, transferred to nitrocellulose, and probed for by antibodies for TPX2, XHRAMM, and γ-tubulin (Sigma).

Approximately 20 μl of glutathione beads (Sigma) were prebound with 125 μg of GST-TPX2 (or GST) in the presence of 5% bovine serum albumin (BSA) in CSF-XB (10 mM K-HEPES [pH 7.7], 100 mM KCl, 1 mM MgCl2, 0.1 mM $CaCl_2$, 50 mM sucrose, 1 mM $MgCl_2$, and 5 mM EGTA). Beads were washed four times in CSF-XB and incubated in 150 μl of CSF. The beads were washed five times with TBS and mixed with 25 μl of 2× sample buffer. Approximately 2 μl of each sample was run on SDS-PAGE, transferred to nitrocellulose, and immunoblotted with antibodies for TPX2 and XRHAMM.

XRHAMM Bead Nucleation Assays

XRHAMM magnetic beads isolated from immunodepletions (as described above) were washed three times with CSF-XB and were diluted in 50 μl of CSF-XB. About 10–15 μl of this bead mixture was added to 200 μl of fresh meiotic *Xenopus* egg extract and incubated for 5 min at 20°C. Then, 10 μm nocodazole and 1 mg/ml RanQ69L(GTP) were added to the extract and incubated for 20 min at 20°C. The beads were then retrieved, washed three times with 4° BRB80, incubated at 37°C in an X-rhodamine-labeled tubulin mix (1 mg/ml), and viewed by fluorescent microscopy for microtubule assembly.

Supplemental Data

Additional Experimental Procedures for this article are available at www.current-biology.com/cgi/content/full/14/20/1801/DC1/.

Acknowledgments

We thank William S. Lane for mass spectrometry and members of the Mitchison lab and M. Shirasu-Hiza, K. Kozminski, B. Brieher, and E.D. Salmon for comments on the manuscript. We thank R. Heald, T. Maresca, Y. Zheng, and J. Walter for antibodies. We thank A. Salic for Ran(Q69L) constructs and A. Straight for the ovary cDNA *Xenopus* library. This work was supported by National Institutes of Health grants to T.J.M. (GM39565) and R.O. (GM20309) and a National Science Foundation Graduate Research fellowship to A.C.G. L.A.C. is supported by postdoctoral fellowship PF-02-095-01-CCG from the American Cancer Society.

Received: June 26, 2004
Revised: August 25, 2004
Accepted: September 9, 2004
Published: October 26, 2004

References

1. Inoue, S., and Ritter, H., Jr. (1975). Dynamics of mitotic spindle organization and function. Soc. Gen. Physiol. Ser. *30*, 3–30.
2. Inoue, S. (1981). Cell division and the mitotic spindle. J. Cell Biol. *91*, 131s–147s.
3. Gaglio, T., Dionne, M.A., and Compton, D.A. (1997). Mitotic spindle poles are organized by structural and motor proteins in addition to centrosomes. J. Cell Biol. *138*, 1055–1066.
4. Cullen, C.F., and Ohkura, H. (2001). Msps protein is localized to acentrosomal poles to ensure bipolarity of Drosophila meiotic spindles. Nat. Cell Biol. *3*, 637–642.
5. Mitchison, T., and Kirschner, M. (1984). Microtubule assembly nucleated by isolated centrosomes. Nature *312*, 232–237.
6. Wilde, A., and Zheng, Y. (1999). Stimulation of microtubule aster formation and spindle assembly by the small GTPase Ran. Science *284*, 1359–1362.
7. Nachury, M.V., Maresca, T.J., Salmon, W.C., Waterman-Storer, C.M., Heald, R., and Weis, K. (2001). Importin beta is a mitotic target of the small GTPase Ran in spindle assembly. Cell *104*, 95–106.
8. Kalab, P., Weis, K., and Heald, R. (2002). Visualization of a Ran-GTP gradient in interphase and mitotic Xenopus egg extracts. Science *295*, 2452–2456.
9. Schatz, C.A., Santarella, R., Hoenger, A., Karsenti, E., Mattaj, I.W., Gruss, O.J., and Carazo-Salas, R.E. (2003). Importin alpha-regulated nucleation of microtubules by TPX2. EMBO J. *22*, 2060–2070.
10. Gaglio, T., Saredi, A., Bingham, J.B., Hasbani, M.J., Gill, S.R., Schroer, T.A., and Compton, D.A. (1996). Opposing motor activities are required for the organization of the mammalian mitotic spindle pole. J. Cell Biol. *135*, 399–414.
11. Wittmann, T., Wilm, M., Karsenti, E., and Vernos, I. (2000). TPX2, A novel Xenopus MAP involved in spindle pole organization. J. Cell Biol. *149*, 1405–1418.
12. Ohi, R., Coughlin, M.L., Lane, W.S., and Mitchison, T.J. (2003). An inner centromere protein that stimulates the microtubule depolymerizing activity of a KinI kinesin. Dev. Cell *5*, 309–321.
13. Lupas, A., Van Dyke, M., and Stock, J. (1991). Predicting Coiled Coils from Protein Sequences. Science *252*, 1162–1164.
14. Lynn, B.D., Li, X., Cattini, P.A., Turley, E.A., and Nagy, J.I. (2001). Identification of sequence, protein isoforms, and distribution of the hyaluronan-binding protein RHAMM in adult and developing rat brain. J. Comp. Neurol. *439*, 315–330.
15. Assmann, V., Jenkinson, D., Marshall, J.F., and Hart, I.R. (1999). The intracellular hyaluronan receptor RHAMM/IHABP interacts with microtubules and actin filaments. J. Cell Sci. *112*, 3943–3954.
16. Hardwick, C., Hoare, K., Owens, R., Hohn, H.P., Hook, M., Moore, D., Cripps, V., Austen, L., Nance, D.M., and Turley, E.A. (1992). Molecular cloning of a novel hyaluronan receptor that mediates tumor cell motility. J. Cell Biol. *117*, 1343–1350.
17. Maxwell, C.A., Keats, J.J., Crainie, M., Sun, X., Yen, T., Shibuya, E., Hendzel, M., Chan, G., and Pilarski, L.M. (2003). RHAMM is

a centrosomal protein that interacts with dynein and maintains spindle pole stability. Mol. Biol. Cell *14*, 2262–2276.
18. Wittmann, T., and Hyman, T. (1999). Recombinant p50/dynamitin as a tool to examine the role of dynactin in intracellular processes. Methods Cell Biol. *61*, 137–143.
19. Paschal, B.M., Holzbaur, E.L., Pfister, K.K., Clark, S., Meyer, D.I., and Vallee, R.B. (1993). Characterization of a 50-kDa polypeptide in cytoplasmic dynein preparations reveals a complex with p150GLUED and a novel actin. J. Biol. Chem. *268*, 15318–15323.
20. Echeverri, C.J., Paschal, B.M., Vaughan, K.T., and Vallee, R.B. (1996). Molecular characterization of the 50-kD subunit of dynactin reveals function for the complex in chromosome alignment and spindle organization during mitosis. J. Cell Biol. *132*, 617–633.
21. Heald, R., Tournebize, R., Blank, T., Sandaltzopoulos, R., Becker, P., Hyman, A., and Karsenti, E. (1996). Self-organization of microtubules into bipolar spindles around artificial chromosomes in Xenopus egg extracts. Nature *382*, 420–425.
22. Bischoff, F.R., Klebe, C., Kretschmer, J., Wittinghofer, A., and Ponstingl, H. (1994). RanGAP1 induces GTPase activity of nuclear Ras-related Ran. Proc. Natl. Acad. Sci. USA *91*, 2587–2591.
23. Zheng, Y., Wong, M.L., Alberts, B., and Mitchison, T. (1995). Nucleation of microtubule assembly by a gamma-tubulin-containing ring complex. Nature *378*, 578–583.
24. Martin, O.C., Gunawardane, R.N., Iwamatsu, A., and Zheng, Y. (1998). Xgrip109: A gamma tubulin-associated protein with an essential role in gamma tubulin ring complex (gammaTuRC) assembly and centrosome function. J. Cell Biol. *141*, 675–687.
25. Moritz, M., Braunfeld, M.B., Guenebaut, V., Heuser, J., and Agard, D.A. (2000). Structure of the gamma-tubulin ring complex: A template for microtubule nucleation. Nat. Cell Biol. *2*, 365–370.
26. Zheng, Y., Wong, M.L., Alberts, B., and Mitchison, T. (1998). Purification and assay of gamma tubulin ring complex. Methods Enzymol. *298*, 218–228.
27. Heald, R., Tournebize, R., Habermann, A., Karsenti, E., and Hyman, A. (1997). Spindle assembly in Xenopus egg extracts: Respective roles of centrosomes and microtubule self-organization. J. Cell Biol. *138*, 615–628.
28. Walczak, C.E., Vernos, I., Mitchison, T.J., Karsenti, E., and Heald, R. (1998). A model for the proposed roles of different microtubule-based motor proteins in establishing spindle bipolarity. Curr. Biol. *8*, 903–913.
29. Merdes, A., Ramyar, K., Vechio, J.D., and Cleveland, D.W. (1996). A complex of NuMA and cytoplasmic dynein is essential for mitotic spindle assembly. Cell *87*, 447–458.
30. Merdes, A., Heald, R., Samejima, K., Earnshaw, W.C., and Cleveland, D.W. (2000). Formation of spindle poles by dynein/dynactin-dependent transport of NuMA. J. Cell Biol. *149*, 851–862.
31. Carazo-Salas, R.E., Guarguaglini, G., Gruss, O.J., Segref, A., Karsenti, E., and Mattaj, I.W. (1999). Generation of GTP-bound Ran by RCC1 is required for chromatin-induced mitotic spindle formation. Nature *400*, 178–181.
32. Eyers, P.A., Erikson, E., Chen, L.G., and Maller, J.L. (2003). A novel mechanism for activation of the protein kinase aurora a. Curr. Biol. *13*, 691–697.
33. Henri, J.F., George, B.A., John, K.N., and Austen, M.A. (2001). World Intellectual Property Organization (WPO) patent WO0121596.
34. Desai, A., Murray, A., Mitchison, T.J., and Walczak, C.E. (1999). The use of Xenopus egg extracts to study mitotic spindle assembly and function in vitro. Methods Cell Biol. *61*, 385–412.
35. Hyman, A., Drechsel, D., Kellogg, D., Salser, S., Sawin, K., Steffen, P., Wordeman, L., and Mitchison, T. (1991). Preparation of modified tubulins. Methods Enzymol. *196*, 478–485.
36. Lohka, M.J., and Masui, Y. (1984). Roles of cytosol and cytoplasmic particles in nuclear envelope assembly and sperm pronuclear formation in cell-free preparations from amphibian eggs. J. Cell Biol. *98*, 1222–1230.
37. Stewart, M., Kent, H.M., and McCoy, A.J. (1998). The structure of the Q69L mutant of GDP-Ran shows a major conformational change in the switch II loop that accounts for its failure to bind nuclear transport factor 2 (NTF2). J. Mol. Biol. *284*, 1517–1527.
38. Maddox, P., Desai, A., Oegema, K., Mitchison, T.J., and Salmon, E.D. (2002). Poleward microtubule flux is a major component of spindle dynamics and anaphase a in mitotic Drosophila embryos. Curr. Biol. *12*, 1670–1674.
39. Field, C.M., Oegema, K., Zheng, Y., Mitchison, T.J., and Walczak, C.E. (1998). Purification of cytoskeletal proteins using peptide antibodies. Methods Enzymol. *298*, 525–541.

Accession Numbers

The GenBank accession number for the XMAP150 sequence reported in this article is AY729653.